Journal of Bioresources and Bioproducts 5 (2020) 211–221

Contents lists available at ScienceDirect

Journal of Bioresources and Bioproducts

journal homepage: www.elsevier.com/locate/jobab

Numerical investigation of thermo-physical properties of non-newtonian fliud in a modelled intestine

S.E. Ibitoye[a,*], I.K. Adegun[a], P.O. Omoniyi[a], T.S. Ogedengbe[b], O.O. Alabi[a]

[a] Department of Mechanical Engineering, University of Ilorin, PMB 1515, Ilorin, Nigeria
[b] Department of Mechanical Engineering, Elizade University, Nigeria

ARTICLE INFO

Keywords:
Axial position
Flow temperature
Flow velocity
Heat transfer
Modelled intestine

ABSTRACT

Several kinds of researches have been conducted on peristaltic flow of non-Newtonian fluid in modelled oesophagus, stomach and intestine. However, further investigation is still needed especially in the area of mechanical shear stress, the influence of inlet temperature and velocity, Nutsselt number and the history of strain rates experienced by fluid particles. This study presents the numerical investigation of thermo-physical properties of non-Newtonian fluid in a modelled intestine. The properties investigated were fluid temperature, velocity, Nutsselt number and wall shear stress. Numerical simulation was performed by solving 3D Navier-Stokes and continuity equations. The intestinal model was drawn by using Autodesk Inventor 2017 while the numerical investigation was conducted by using ANSYS FLUENT 16.0. The Computational Fluid Dynamics solver employs the Finite Element Method (FEM) to discretize the governing equations. Chyme, Hibiscus Sabdariffa Roselle (Sobo), Soymilk (Soya) and Pap (Ogi) were the working fluids used for the investigation. Analyses of the results showed that the variation of fluid temperature and heat transfer with axial position across the length of intestinal model were not significantly influenced by the variation of the inlet velocity. Expansion of the model about the pulsating part enhanced heat transfer and nutrient delivery to the intestinal walls. Variation of the inlet velocity did not affect the average Nutsselt number. Chyme and Sobo had the highest and lowest Nutsselt number, respectively. Sobo displayed the best fluid properties considering flow behaviour while Soya displayed the best properties for thermal history. The results presented in this study are of countless importance in medical, paramedical, engineering applications, thermoregulation system, thermotherapy, and biomedical disciplines, where analyses and investigation of gastrointestinal tract history can be understudied.

1. Introduction

Digestion is an intricate process that includes the breakdown and transformation of food into elements that can be absorbed by the body for effective human growth (Ehsan et al., 2020), and the process initiates from the mouth and ends in the large intestine. The anus is where the end products of undigested fluids are being eliminated from the body. From the biological point of view, movement of food or Chyme from the mouth to the anal passage is as a result of proper nutrition (Adegun, 2020). This involves several forces and reactions that lead to three important motions within the gastrointestinal tract, which are the segmentation, peristalsis and pendular movements (Adegun, 2020; Hayat et al., 2017). The pendular movement does not propel the Chyme along the intestinal tract but moderately mixes and chops the contents so that it can be properly digested, while peristalsis and segmentation are a sequence of

* Corresponding author.
E-mail address: ibitoyeesegun@gmail.com (S.E. Ibitoye).

https://doi.org/10.1016/j.jobab.2020.07.007

Available online 29 July 2020
2369-9698/© 2020 The Author(s). Published by Nanjing Forestry University. This is an open access article under the CC BY-NC-ND license. (http://creativecommons.org/licenses/by-nc-nd/4.0/)

wave-like muscular contractions that drive the Chyme via the small intestine. The human small intestine is a highly multifaceted hollow organ positioned at the upper part of the intestinal tract and it consists of the intestinal epithelium, submucosa, muscularis mucosa, lamina propria and serosa (Chen et al., 2017; Schulte et al., 2019). Food in liquid form naturally gets to the stomach before solid and semi-solid food, and as a result, there is a time difference in the rate at which food at different states leaves the stomach, but the small intestine transports foods in all states at about the same rate. It takes approximately 150 min for half the solids and liquid Chyme of the same caloric density to pass through the small bowel for energy to be available for the body (Fonseca, 2011; Hari et al., 2012).

The intricate mechanical behaviours of physiological fluids can be categorized as either Newtonian or non-Newtonian fluids (Tripathi and Anwar Bég, 2013; Dejam, 2018; Adegun, 2020). The viscosity of a Newtonian fluid is independent of pressure while non-Newtonian viscosity changes when pressure is applied. Recently, researchers have focused on their resources towards non-Newtonian fluids due to their enormous technological and industrial applications (Alokaily, 2017; Cortez et al., 2018; Dejam, 2018; Alokaily et al., 2019). The fluids used in petrochemical, chemical and food industries are non-Newtonian (Farooq et al., 2019).

It has previously been established that fluid motion enhances heat transfer, since it brings hotter and cooler chunks of fluid into contact, initiating higher rates of conduction at a greater number of sites in a fluid (Mernone 2000; Srivastava, 2007; Nadeem et al., 2012). However, the rate of heat transfer through a fluid is much higher by convection than conduction. Studies have shown that convection heat transfer strongly depends on the fluid properties such as dynamic viscosity, thermal conductivity, density, specific heat, as well as the fluid velocity (Ellahi et al., 2014; Cengel and Ghajar, 2015). Heat transfer is the exchange of the sensible and latent forms of internal energy between two media as a result of a temperature difference. Heat transfer in tube flow occurs from the hot to cold particles by conduction when the fluid layers are static and by convection when the fluid is in motion. Convection heat transfer is complicated by the fact that it involves fluid motion as well as the heat of conduction (Marciani et al., 2001; Adegun, 2020). The ratio of heat flux by convection to the heat flux by conduction is determined by a dimensionless number, called Nusselt number.

The functional attributes of many traditional foods are being discovered, while new food products are being developed with beneficial components. This is due to the new techniques which can increase the thermal efficiency of working fluid and thus reduce overall health crises (Abrar et al., 2020).

Many researchers have applied mathematical, computational and numerical techniques to study the peristaltic flow of fluid in the human digestive system. Alokaily et al. (2019) studied the characterization of peristaltic flow during the mixing process in a modelled human stomach. Geometric model was implemented into the open-source code Open-FOAM while parametric study was performed on wave width, fluid viscosity and wave speed. Retropulsive jet induced near the recirculation and pylorus between pairs of consecutive antral contraction waves were investigated based on the selected parameters. It was concluded that the mixing efficiency increased with a decrease in viscosity and wave width. It was suggested that further studies should be conducted on the disintegration of food particles due to mechanical stresses and strain rates experienced by fluid particles. Adegun (2020) performed numerical simulation on laminar flow of non-Newtonian fluids in a rhythmical non-permeable medium. The study presented the flow of orange juice, chyme and watermelon juice via a modelled oesophagus. ANSYS FLUENT, SolidWorks and Computational Fluid Dynamics technique were adopted for this study. It was reported that the highest pressure built up in the tube was observed with orange juice while water melon juice had the least presure. The study was concluded by recommending flow velocity of 0.005 m/s for effective fluid flow and heat transfer in a tube.

In 2015, Tripathi et al. (2015) simulated peristaltic viscoelastic bio-fluid flow in asymmetric porous media using differential transform method. Dynamics mathematical model was developed to study the peristaltic flow of non-Newtonian physiological liquid in a 2-D asymmetric channel and the influence of fractional parameters (volumetric flow rate, pressure difference and wall friction force) on peristaltic flow characteristics were computed. They concluded that the fractional parameter had a significant influence on the flow of physiological fluid.

The current investigation is conducted to improve the previous analytical and numerical works of (Ellahi, et al., 2014; Tripathi et al., 2015; Tripathi et al., 2016; Ismail, 2017; Adegun, 2020). This study seeks to advance knowledge on peristaltic bio-fluid using Computational Fluid Dynamics and 3D modelling techniques. An intestinal model with different geometries have been conducted, and these include curved tube (Tripathi et al., 2016), straight pipe (Ismail, 2017) and non-uniform rectangular duct (Ellahi et al., 2014) among other geometries. Therefore, this study is conducted using a non-uniform circular tube. Ismail (2017) reported that the presence of villi (expansion) in the small intestine enhances nutrient absorption by the intestinal walls, however, further study is required to investigate the heat transfer characteristics of villi. Several numerical and computational solver/tools have been utilized to critically investigate fluid flow in modelled intestine. These include Computation Fluid Dynamics Solver (Ansys Fluent, OpenFoam, MAPLE17 Numerical Quadrature, COMSOL MultiPhysics, etc.) and CAD tools (Solid Works, Autodesk Inventor, AutoCAD, Corel Draw etc.).

This study also investigated how the structuring of foods can influence the delivery of nutrients to the wall of the small intestine using numerical techniques. It investigates and establishes whether villi could significantly influence intestinal walls heat transfer characteristics. This will help to predict the in-vivo performance of food after ingestion and establish the physiological and physico-chemical factors affecting chemical reaction and delivery processes in the human body. The general sketch of the problem is shown in Fig. 1. This article is presented in the following outline: first, methodology, where the computational model and governing equations were developed. The results and discussion are then presented and lastly, the summary and conclusions.

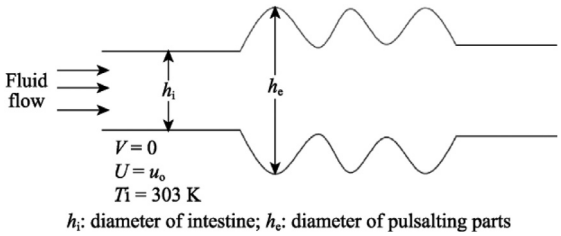

Fig. 1. General sketch of problem.

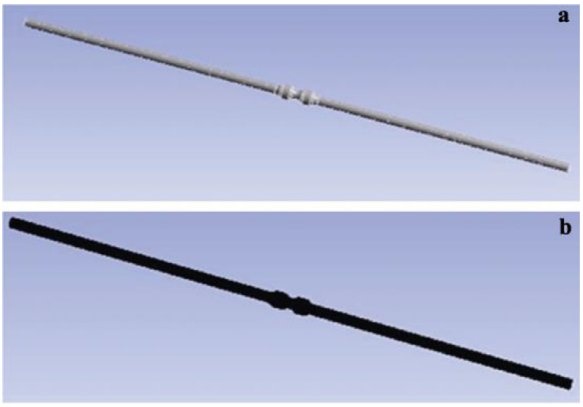

Fig. 2. Modeled intestine (a) and mesh generated domain of intestine (b).

Table 1
Thermo-physical properties of fluids considered in this study.

Fluid	Density (kg/m^3)	Viscosity (Pa•s)	Specific heat capacity (J/(kg•K))	Thermal conductivity (W/(m•K))
Chyme	1 000	1.000	4 180	0.600
Pap (Ogi)	1 024	1.095	1 840	0.536
Soymilk (Soya)	920	0.95	3 970	0.501
Hibiscus sabdariffa roselle (Sobo)	800	0.316	2 470	0.491

Source: Berk, 2013

2. Methodology

2.1. Fluid property

The thermo-physical properties of the fluid used are presented in Table 1. This is comprised of density, viscosity, specific heat capacity and thermal conductivity.

2.2. Computational tool and model

The research focuses on incompressible and viscous fluid flow through the mouth to the lower part of the gastrointestinal tract (GIT) and small intestine. AUTODESK INVENTOR 2017 commercial version was used for the computational modelling of the human intestine as well as the steady flow field generated inside the modelled intestine. The movement of the contraction waves within the alimentary canal was simulated using a commercial version of CFD solver, ANSYS FLUENT 16.0. Navier-stokes equations of fluid flow with deformed boundary walls were used for the model. Fig. 2 shows the mesh generated domain and the modelled intestine.

2.3. Governing equation

The model is governed by the continuity equation and Navier-Stokes equations with the following assumptions: (i) The flow is a laminar natural convection; (ii) It is assumed to be a steady-state hydrodynamics incompressible fluid flow; (iii) The inlet temperature is 303 K; (iv) The velocity profile is fully developed in the model; (v) The velocity along the radial direction is assumed to be zero, i.e., velocity along the radial direction is insignificant when compared with axial velocity; (vi) The effect of gravity is neglected; (vii) No slip boundary condition at the walls is employed; (viii) The thermal boundary condition of constant heat flux is applied.

2.4. Continuity equation

The continuity equation that governs the numerical model is presented in Equation (1):

$$\frac{\partial U_r}{\partial r} + \frac{1}{r}\frac{\partial U_\phi}{\partial \phi} + \frac{\partial U_x}{\partial x} = 0 \tag{1}$$

where U_x is non-zero velocity component, r is non-dimensional radial coordinate, ϕ is non-dimensional azimuthal coordinate, and x is non-dimensional axial coordinate, thus, $U_r = U_\phi = 0$. There, Equation (1) is reduced to $\partial U_x/\partial x = 0$. It confirms that U_x does not depend on the radial component of the tube which implies a thinned wall tube and also $U_x = U_x(r) = 0$ is the same for all values of x, thus $U_x = U_x(r)$.

2.5. Momentum equation

Radial direction:

$$\rho\left(\frac{\partial U_r}{\partial t} + U_r\frac{\partial U_r}{\partial r} + \frac{U_\phi}{r}\frac{\partial U_r}{\partial \phi} + U_x\frac{\partial U_r}{\partial x} + \frac{{U_\phi}^2}{r}\right) = \rho g_r - \frac{\partial \rho}{\partial r} + \mu\left[\begin{array}{l}\frac{\partial^2 U_r}{\partial r^2} + \frac{1}{r^2}\frac{\partial^2 U_r}{\partial \phi^2} + \frac{\partial^2 U_r}{\partial x^2} + \\ \frac{1}{r}\frac{\partial U_r}{\partial r} - \frac{2}{r^2}\frac{\partial U_\phi}{\partial \phi} - \frac{U_r}{r^2}\end{array}\right] \tag{2}$$

where ρ is fluid desity, t is time, μ is dynamic fluid viscosity, and g is acceleration due to gravity.

Azimuthal direction:

$$\rho\left(\frac{\partial U\phi}{\partial t} + U_r\frac{\partial U_\phi}{\partial r} + \frac{U_\phi}{r}\frac{\partial U_\phi}{\partial \phi} + U_x\frac{\partial U_\phi}{\partial x} + \frac{U_\phi^2}{r}\right) = \rho g_\phi - \frac{\partial \rho}{\partial \phi} + \mu\left[\begin{array}{l}\frac{\partial^2 U_\phi}{\partial r^2} + \frac{1}{r^2}\frac{\partial^2 U_\phi}{\partial \phi^2} + \frac{\partial^2 U_\phi}{\partial x^2} + \\ \frac{1}{r}\frac{\partial U_\phi}{\partial r} + \frac{2}{r^2}\frac{\partial U_r}{\partial \phi} - \frac{U_\phi}{r^2}\end{array}\right] \tag{3}$$

Axial direction:

$$\rho\left(\frac{\partial U_x}{\partial t} + U_r\frac{\partial U_x}{\partial r} + \frac{U_\phi}{r}\frac{\partial U_x}{\partial \phi} + U_x\frac{\partial U_x}{\partial x}\right) = \rho g_x - \frac{\partial \rho}{\partial x} + \mu\left[\frac{\partial^2 U_x}{\partial r^2} + \frac{1}{r^2}\frac{\partial^2 U_x}{\partial \phi^2} + \frac{\partial^2 U_x}{\partial x^2} + \frac{1}{r}\frac{\partial U_x}{\partial r}\right] \tag{4}$$

Substituting $U_r = U_\phi = 0$ and $\partial U_x/\partial x = 0$ into equations (2) and (3), gives $\partial \rho/\partial r = 0$ and $\partial \rho/\partial_\phi = 0$. $\partial \rho/\partial r = 0$ and $\partial \rho/\partial_\phi = 0$ show that pressure depends only on axial direction and imposing steady state condition yields $\partial U_x/\partial t = 0$.

$$\frac{\partial \rho}{\partial x} = \rho g_x + \mu\left[\frac{\partial^2 U_x}{\partial r^2} + \frac{1}{r^2}\frac{\partial^2 U_x}{\partial \phi^2} + \frac{\partial^2 U_x}{\partial x^2} + \frac{1}{r}\frac{\partial U_x}{\partial r}\right] \tag{5}$$

Neglecting gravitational effect, Equation (6) is the momentum transport equation for the model.

$$\frac{\partial \rho}{\partial x} = \mu\left[\frac{\partial^2 U_x}{\partial x^2}\right] \tag{6}$$

2.6. Energy equation

The energy transport equation for a steady for flow is:

$$k\frac{\partial^2 T}{\partial r^2} + \frac{k}{r^2}\frac{\partial^2 T}{\partial \phi^2} + \frac{\partial^2 T}{\partial x^2} + \frac{k}{r}\frac{\partial T}{\partial r} + \phi_{(i)} = \rho C_p\left[U_r\frac{\partial T}{\partial r} + U_\phi\frac{\partial T}{\partial \phi} + U_x\frac{\partial T}{\partial x}\right] \tag{7}$$

where k is thermal conductivity, T is fluid temperature, C_p is specific heat capacity, $\phi_{(i)}$ is viscous dissipation term.

Eliminating the viscous dissipation term $\phi_{(i)}$:

$$\frac{\partial^2 T}{\partial x^2} + \frac{1}{r}\frac{\partial T}{\partial r} = \frac{\rho C_p}{k}\left[U_x\frac{\partial T}{\partial x}\right] \tag{8}$$

Energy Transport Equation for flow within the tube is presented in Equatoin (9):

$$\frac{\partial^2 T}{\partial x^2} = \frac{U_x}{\alpha}\frac{\partial T}{\partial x} \tag{9}$$

where $\alpha = (k/\rho C_p)$, constant.

2.7. Flow in porous medium

Since the intestine is a porous medium and the flow is a laminar natural convection, which is also assumed to be a steady-state hydrodynamics incompressible fluid flow. Therefore, the Darcy's law is applied and is presented in Equation (10):

$$K = \frac{\mu q L}{\Delta P} \tag{10}$$

where P is pressure, L is length of flow, q is fluid flow rate.

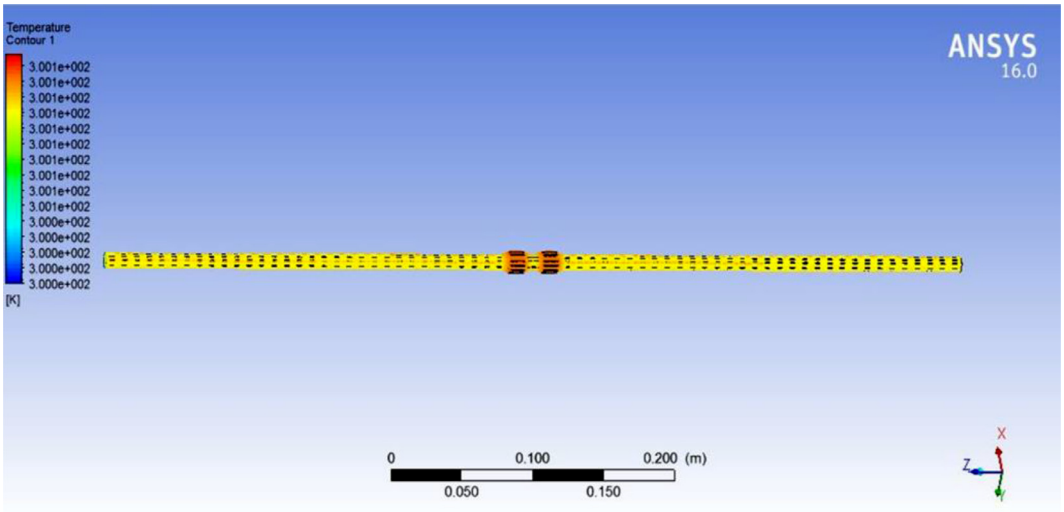

Fig. 3. Temperature flow profile across length of intestinal model.

2.8. Shear stress

The relationship between the shear stress and shear rate for a power law non-newtonian fluid is presented in Equation (11):

$$\sigma = H\gamma^n \tag{11}$$

where σ is shear stress, γ is shear rate, H is consistency of the power-law fluid, and n is power-law index.

2.9. Evaluation of mean Nusselt number

Nusselt number represents the rate of heat transfer across the wall. The tendency of the model and the pulsating part in providing heat transfer augmentation is critically examined and governed by Equation (12):

$$h(\phi, x) = \frac{q(\phi, x)}{T_w(\phi, x) - T_b(x)}; N_u = \frac{h(x)d_h}{k} \tag{12}$$

where T_w is wall temperature, T_b is bulk fluid temperature, q is fluid flow rate, and d_h is hydraulic diameter of intestinal model.

3. Results and Discussion

3.1. Temperature

Figures 3 and 4 show the temperature contour profile across the entire length of the fluid domain and pulsating part of the modelled intestine, respectively. Figs. 5–8 show the temperature contour along the duct of the intestinal model. It was observed from Figs. 9–12 that the temperature increases from the inlet to the outlet of the model for all the fluids samples. This rise in temperature as the fluid moves towards the outlet is as a result of an expansion at the pulsating section of the intestine. These heats are being transferred to other body fluids which at times result in sweating and heat dissipation through the skin. The expansion and the presence of villi do not only enhance nutrient absorption as reported by Ismail (2017), it could also be observed that it improves heat transfer characteristics of the intestinal walls. However, the results are shown in Figs. 9–12, the variation of the temperature of the flowing fluid and heat transfer with axial position across the length of intestinal model was not significantly affected by the variation of the inlet velocity, and that was the reason why the temperature profiles of all the fluids align on the same line curve for all the inlet velocities (Figs. 9–12). A change in temperature was also observed at the pulsating part of the model and latter increased to the end. This was due to the change in surface area as a result of peristaltic movement in the intestine which enhances fluid delivery to the intestinal walls.

3.2. Nusselt number

Figures 13–16 show the variation of Nutsselt number along with the axial position of the intestinal model for different inlet velocity. Chyme and Sobo had the highest and lowest Nutsselt number, respectively. It was observed that Ogi, Chyme and Soya displayed a similar pattern of heat transfer while Soya exhibited the best heat transfer followed by Ogi. The trend of the plots shows that Soya and Ogi can compete favourably well with Chyme in the human body, hence recommended for a patient under medication

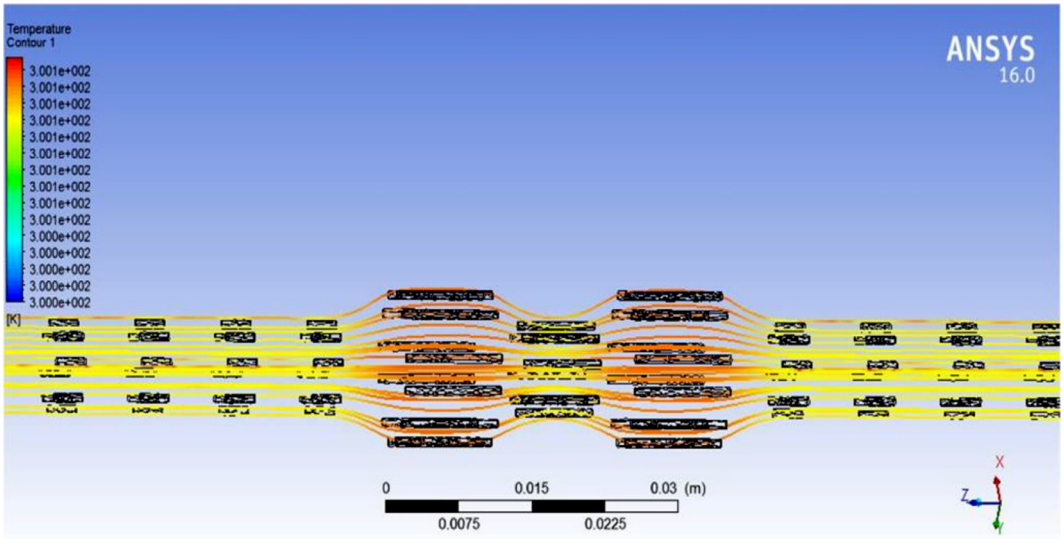

Fig. 4. Temperature flow profile for pulsating part of intestinal model.

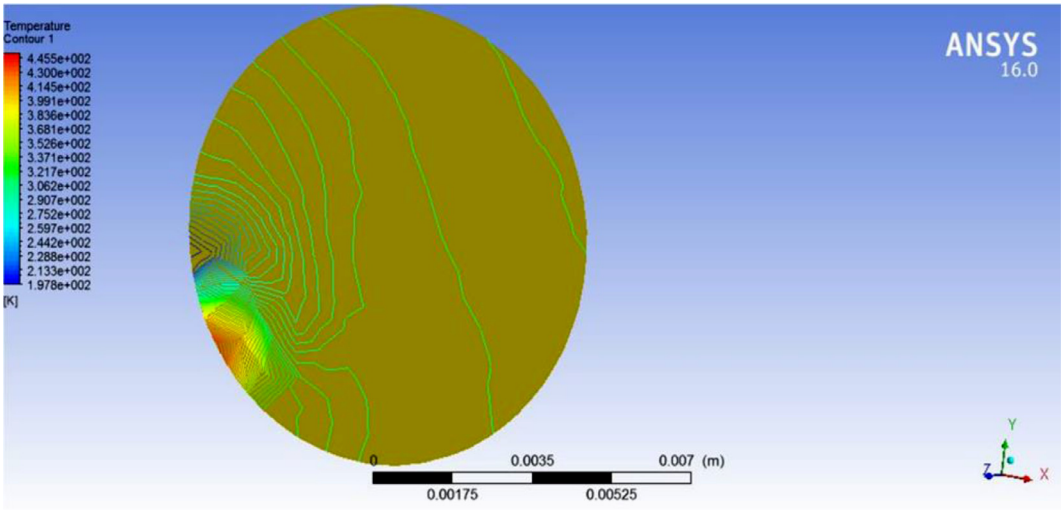

Fig. 5. Temperature flow profile along cross duct section at 0.08 m of intestinal model.

for better nutrient delivery and quick recovery. The result shows that Sobo does not exhibit good heat transfer property and does not compete favourably with the characteristics of Chyme. With critical analysis of Figs. 13–16, it was observed that variation of the inlet velocity does not obviously influence the average Nutsselt number and heat transfer characteristics of all the fluids considered in the study. The trend of the curves was strongly in line with what was observed within the temperature profiles (Figs. 9–12). It could be found that Sobo is the best fluid considering flow behaviour while Soya is the best for thermal history.

3.3. Shear stress

The variation of average wall shear stress with axial position along the length of the intestinal model is shown in Fig. 17. As shown in Fig. 17, wall shear stress decreases to the length of 0.1 m before it becomes constant and decreases at the pulsating parts of the model. Ogi and Sobo present the highest and the lowest wall shear stress, respectively. Ogi has the highest wall shear along the length of the model followed by Chyme. The shear stress and shear strain relationship do not pass through the origin and this is an indication that the fluids under investigation are non-Newtonian (Fig. 18). For non-Newtonian fluid, viscosity is not constant and the shear stress is imparted onto the boundary as a result of the loss of velocity (Tanner, 2014).

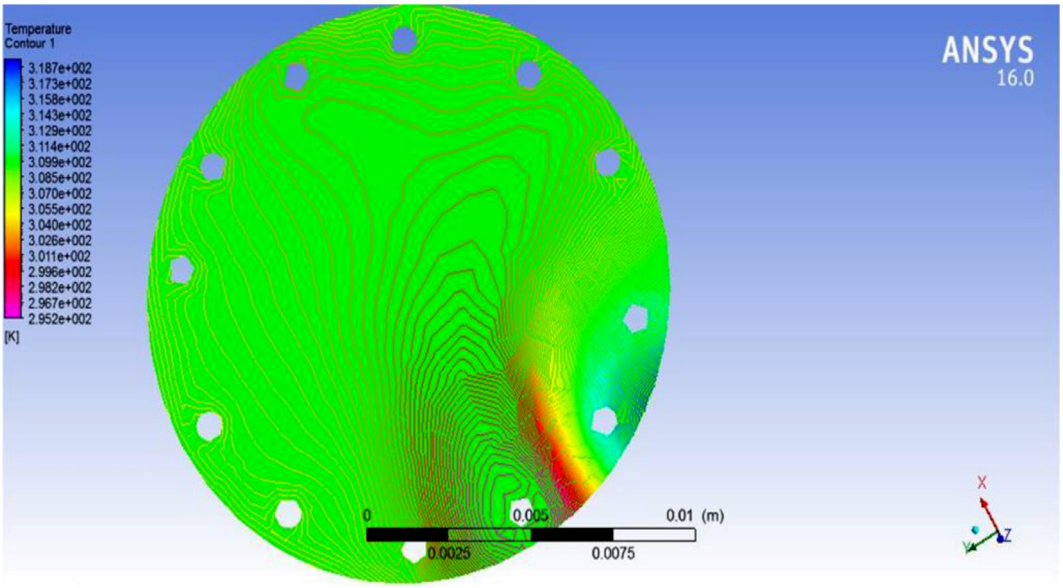

Fig. 6. Temperature flow profile along cross duct section at 1.1 m of intestinal model.

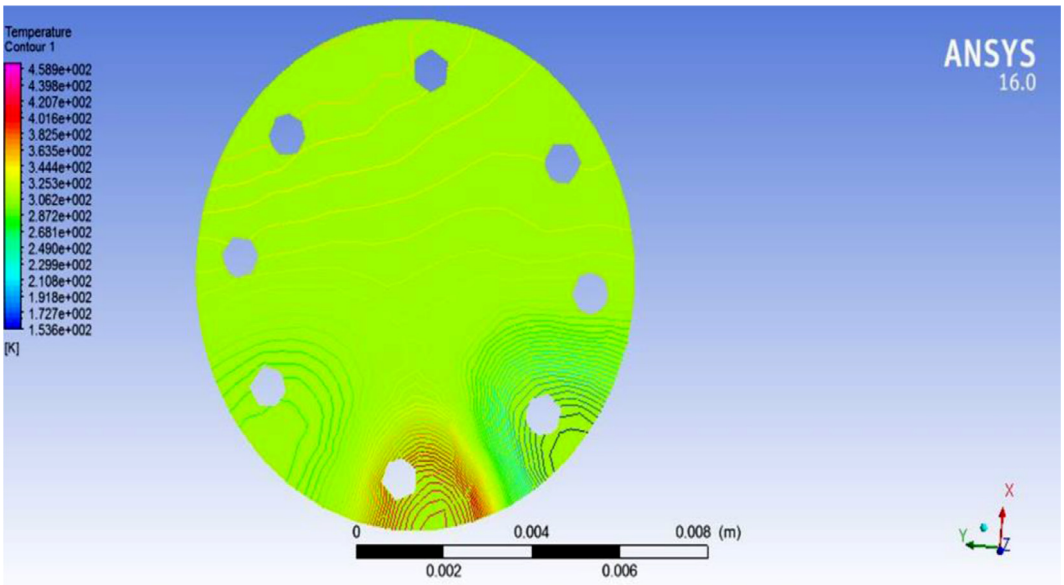

Fig. 7. Temperature flow profile along cross duct section at 1.5 m of intestinal model.

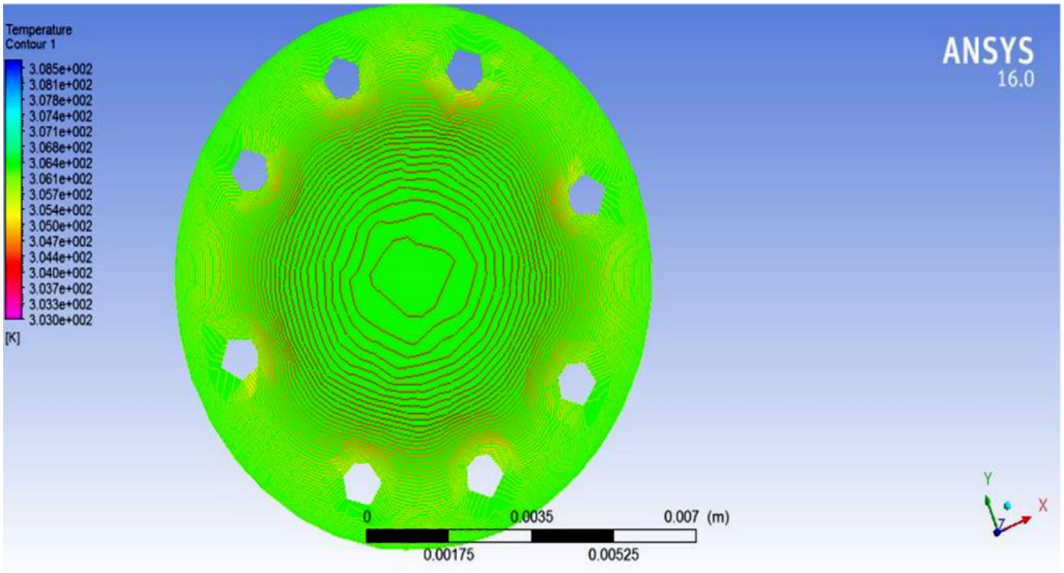

Fig. 8. Temperature flow profile along cross duct section at 2.3 m of intestinal model.

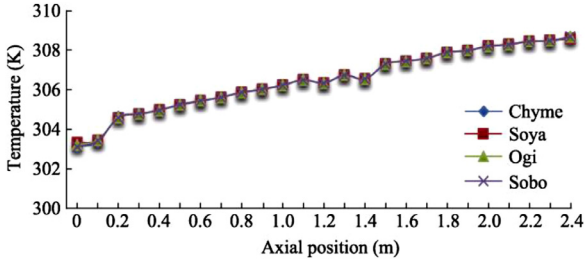

Fig. 9. Variation of flow temperature with axial position across length of intestinal model for inlet velocity of 0.005 m/s.

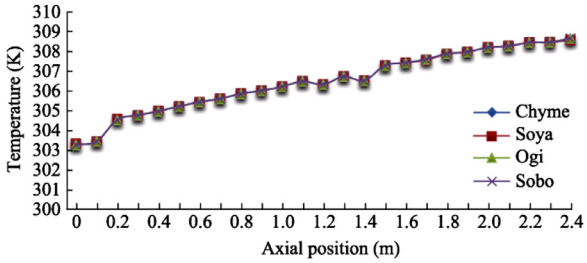

Fig. 10. Variation of flow temperature with axial position across length of intestinal model for inlet velocity of 0.01 m/s.

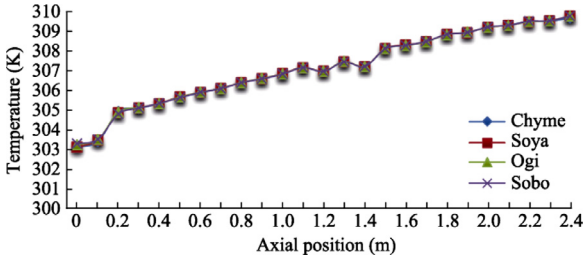

Fig. 11. Variation of flow temperature with axial position across length of intestinal model for inlet velocity of 0.015 m/s.

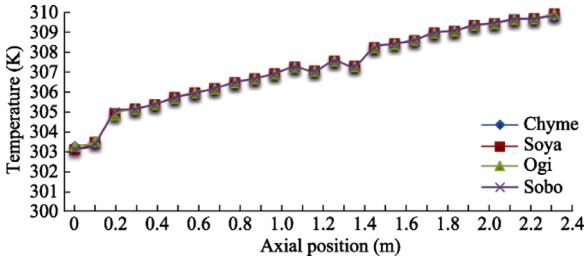

Fig. 12. Variation of flow temperature with axial position across length of intestinal model for inlet velocity of 0.02 m/s.

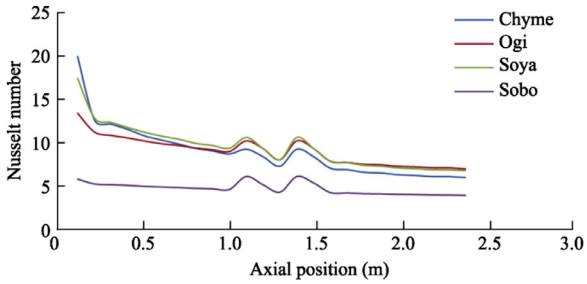

Fig. 13. Variation of Nusselt number along with axial position of intestinal model for different fluids at an inlet velocity of 0.005 m/s.

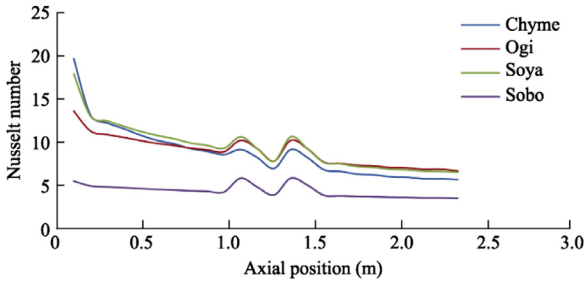

Fig. 14. Variation of Nusselt number along with axial position of intestinal model for different fluids at an inlet velocity of 0.01 m/s.

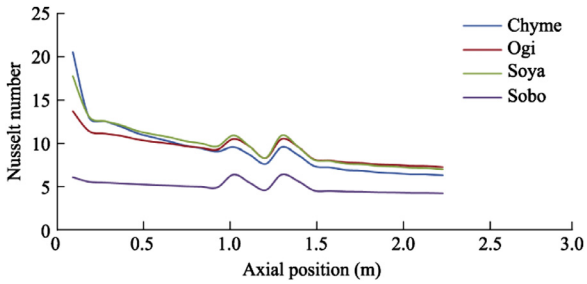

Fig. 15. Variation of Nusselt number along with axial position of intestinal model for different fluids at an inlet velocity of 0.015 m/s.

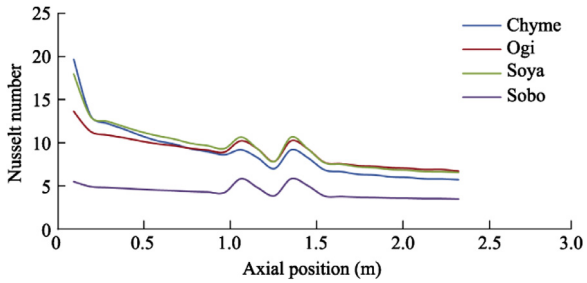

Fig. 16. Variation of Nusselt number along with axial position of intestinal model for different fluids at an inlet velocity of 0.02 m/s.

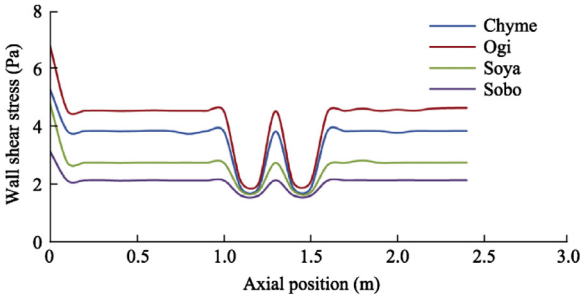

Fig. 17. Variation of average wall shear stress with axial position along length of intestinal model.

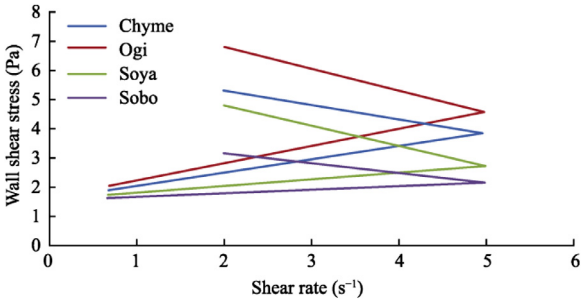

Fig. 18. Variation of shear stress with shear rate along length of intestinal model.

4. Summary and Conclusions

Numerical investigation of a laminar viscous fluids flow in a rhythmical porous medium within the range of different inlet velocities were carried out using four different food samples (Chyme, Ogi, Soya and Sobo) as working fluids. The effects of temperature, wall shear stress, and Nusselt number on nutrient delivery to the wall intestine were investigated. It could be inferred from the study that Villi does not only enhance nutrient absorption by the intestinal walls, it also improves intestinal wall heat transfer properties. Expansion along the model about the pulsating part enhances heat transfer and nutrient delivery to the intestinal walls. Soya and Ogi can function in place of Chyme in the human body, therefore, they are recommended for a patient under medication for better nutrient delivery and quick recovery. The trend of the curves shows that the four fluids considered for the investigation are non-Newtonian. The peristaltic force is responsible for the passage of all the fluids from inlet to the outlet of the modelled intestine. This study expands understanding on heat transfer, shear stress, velocity of fluid flow in human intestine and delivery of nutrient to the intestinal wall. However, further studies should be done on non-Newtonian fluid, especially on the variation of inlet pressure and Reynolds number on fluid flow Phenomena as related to nutrient delivery in the small intestine.

References

Abrar, M.N., Sagheer, M., Hussian, S., 2020. Thermodynamics analysis of Joule heating and internal heat source over an inclined ciliated tube. Phys. A: Stat. Mech. Appl. 549, 123983.

Adegun, I.K., 2020. The one hundred and ninety-third (193rd) inaugural lecture: god the creator, man the manipulator: the journey so far in engineering manipulation of fluids and geometries for human life. University of Ilorin Press, Ilorin, Kwara State, Nigeria.

Alokaily, S., 2017. Modeling and simulation of the peristaltic flow of Newtonian and non-Newtonian fluids with application to the human body. Department of Mathematical Sciences, Michigan Technological University, Michigan.

Alokaily, S., Feigl, K., Tanner, F.X., 2019. Characterization of peristaltic flow during the mixing process in a model human stomach. Phys. Fluids 31, 103105.

Berk, Z., 2013. A volume in food science and technology. Israel Institute of Technology, Israel.

Cengel, Y.A., Ghajar, A.J., 2015. Heat and Mass Transfer: Fundamentals and Applications, 8th ed. Mc Graw-Hill Education, New York.

Chen, Y., Zhou, W.D., Roh, T., Estes, M.K., Kaplan, D.L., 2017. In vitro enteroid-derived three-dimensional tissue model of human small intestinal epithelium with innate immune responses. PLoS One 12, e0187880.

Cortez, A.R., Poling, H.M., Brown, N.E., Singh, A., Mahe, M.M., Helmrath, M.A., 2018. Transplantation of human intestinal organoids into the mouse mesentery: a more physiologic and anatomic engraftment site. Surgery 164, 643–650.

Dejam, M., 2018. Dispersion in non-Newtonian fluid flows in a conduit with porous walls. Chem. Eng. Sci. 189, 296–310.

Ehsan, T., Anjum, H.J., Asghar, S., 2020. Peristaltic flows: a quantitative measure for the size of a bolus. Phys. A: Stat. Mech. Appl. 553, 124211.

Ellahi, R., Mubashir Bhatti, M., Vafai, K., 2014. Effects of heat and mass transfer on peristaltic flow in a non-uniform rectangular duct. Int. J. Heat Mass Transf. 71, 706–719.

Farooq, S., Khan, M.I., Hayat, T., Waqas, M., Alsaedi, A., 2019. Theoretical investigation of peristalsis transport in flow of hyperbolic tangent fluid with slip effects and chemical reaction. J. Mol. Liq. 285, 314–322.

Fonseca, M.R.J., 2011. An engineering understanding of the small intestine. the University of Birmingham, UK.

Hari, B., Bakalis, S., Fryer, P., 2012. Computational modeling and simulation of the human duodenum. University of Birmingham, Birmingham, pp. 1–6.

Hayat, T., Ahmed, B., Abbasi, F.M., Alsaedi, A., 2017. Hydromagnetic peristalsis of water based nanofluids with temperature dependent viscosity: a comparative study. J. Mol. Liq. 234, 324–329.

Ismail, A.A., 2017. Peristaltic flow of some selected food supplements in a modelled oesophagus. Mechanical. University of Ilorin, Nigeria.
Marciani, L., Gowland, P.A., Spiller, R.C., Manoj, P., Moore, R.J., Young, P., Fillery-Travis, A.J., 2001. Effect of meal viscosity and nutrients on satiety, intragastric dilution, and emptying assessed by MRI. Am. J. Physiol.Gastrointest. Liver Physiol. 280, G1227–G1233.
Mernone, A.V., 2000. A mathematical study of peristaltic transport of physiological fluids. Adelaide: Adelaide of University, Department of Applied Mathematics.
Nadeem, S., Ashiq, S., Ali, M., 2012. Williamson fluid model for the peristaltic flow of chyme in small intestine. Math. Probl. Eng. 2012, 1–18.
Schulte, L., Hohwieler, M., Müller, M., Klaus, J., 2019. Intestinal organoids as a novel complementary model to dissect inflammatory bowel disease. Stem Cells Int. 2019, 1–15.
Srivastava, V.P., 2007. Effects of an inserted endoscope on chyme movement in small intestine—A theoretical model. Appl. Appl. Math. (AAM): Int. J. 2, 79–91.
Tanner, R.I., 2014. Engineering rheology., 2nd ed. Oxford University Press, UK.
Tripathi, D., Akbar, N.S., Khan, Z.H., Bég, O.A., 2016. Peristaltic transport of bi-viscosity fluids through a curved tube: a mathematical model for intestinal flow. Proc. Inst. Mech. Eng. Part H: J. Eng. Med. 230, 817–828.
Tripathi, D., Anwar Bég, O., 2013. Peristaltic propulsion of generalized Burgers' fluids through a non-uniform porous medium: a study of chyme dynamics through the diseased intestine. Math. Biosci. 248, 67–77.
Tripathi, D., Bég, O.A., Gupta, P.K., Radhakrishnamacharya, G., Mazumdar, J., 2015. DTM simulation of peristaltic viscoelastic biofluid flow in asymmetric porous media: a digestive transport model. J. Bionic Eng. 12, 643–655.